Adaptive Quasi-Fixed-Time Integral Terminal Sliding Mode Control for Nonlinear Systems

Zhangzhen Zhu, Yongliang Lin and Yu Zhang, *Member, IEEE*

Abstract—This brief proposes an adaptive quasi-fixed-time integral terminal sliding mode control, in order to solve the stabilization problem for a class of invertible nonlinear systems with unknown varying perturbations. The proposed method can drive the sliding manifold into a predefined vicinity of equilibrium and estimate the bound of the state-dependent perturbation in quasi-fixed-time despite the large initial state errors. Besides, the state variable also converges in quasi-fixed-time due to the geometric homogeneous property of the designed sliding manifold. Furthermore, a novel nonsingular adaptive layer function is proposed and the respective control is completely chattering-free, Lipschitz continuous and no gain overestimation exists, which is critical to practical applications under measurement noises. Finally, the superiority of the method is validated through simulation and a permanent magnet synchronous motor control experiment.

Index Terms—Terminal sliding mode control (TSM), adaptive law, fixed-time stability, robust control.

I. INTRODUCTION

Sliding mode control (SMC) is recognized as one of the most successful control methods due to its fast convergence and insensitivity to disturbances [1]. Although traditional SMC has been studied extensively for over 60 years, it requires the actuator to switch infinitely fast to enforce the ideal sliding motion which usually results in damage to the actuator and even excites high-frequency unmodeled dynamics. In recent years, many improved methodologies such as chattering-free terminal SMC (TSM) [2], intermittent SMC [3] and the fixed-time SMC [4], have been proposed to solve the chattering phenomenon, save the control effort and deal with the fixed-time stability respectively. Besides, a high-order SMC (HOSMC) approach is proposed in [5] to mitigate the chattering phenomenon and accomplish the finite-time convergence simultaneously.

Nevertheless, both these improvements require the prior information of the lumped perturbation and the switch gain overestimation is inevitable to overcome the mismatched perturbation. Meanwhile, in many applications containing measurement noises and state-dependent disturbances, HOSMC is not that efficient compared with the conventional SMC [6]. Hence, in recent years, attention has been concentrated on the adaptive SMC to estimate these mismatched perturbations

TABLE I: Comparisons Between SMC Literature.
$\star$: Whether the control input u is Lipschiz continuous.

Literature	Convergence	Continuous*	System Order	Perturbation Info.
[10]	Asymptotic	No	Arbitrary	No requirement
[7], [13]	Finite-Time	No	Arbitrary	No requirement
[2]	Finite-Time	No	Arbitrary	Need
[4], [14]	Fixed-Time	No	Second	Need
[17]	Fixed-Time	No	Arbitrary	Need
This brief	Quasi-Fixed	Yes	Arbitrary	No requirement

online adaptively [7]–[9]. In summary, there exist three types of adaptive SMC:

1) [10], [11]: Increasing the switch gain monotonically until the sliding manifold converges.
2) [7]: Increasing the switch gain monotonically and decreasing the gain when the sliding manifold converges into the predefined boundary layer.
3) [12]: Equivalent control to ensure the switch gain is as small as possible to alleviate the chattering, while still large enough to compensate the lumped perturbations.

Chattering phenomena exist in type 1, 2 and in general, these methods only make sense in theoretical concepts. Meanwhile, non-consideration of the state-dependent perturbation may lead to instability [13]. The equivalent control in type 3 is free of chattering. However, the perturbation is assumed to be an unknown constant that is independent of the system state and different cases are derived which is hard for implementation.

In addition to the mismatched perturbation problems above, many practical applications require robust strict finite-time convergence such as space-station docking and applications in power systems [14]. These finite-time convergence tasks cannot be realized utilizing the conventional SMC [1] and fortunately, thanks to the geometric homogeneous property [15] and theorem in [16], the finite-time, even fixed-time convergence can be realized. Several important finite or fixed-time articles are listed in Table I for a clear comparison.

Motivated by the aforementioned problems, this brief intends to solve the four major issues listed in Table I simultaneously, i.e., fixed-time convergence, Lipschitz continuous controller design, arbitrary-order nonlinear system stabilization, and state-dependent perturbation online estimation.

Specifically, the main contribution of this brief can be summarized as the following aspects.

1) An adaptive quasi-fixed-time integral terminal sliding mode control, coined as AFITSM, is proposed to stabilize the perturbed nonlinear system (later see (1)) and estimate the bound of the state-dependent perturbation in quasi-fixed-time, despite the co-existence of model un-

certainty and exogenous disturbance. Meanwhile, there's no requirement for their derivative information.

2) A novel nonsingular adaptive layer function is designed and the controller is completely chattering-free and Lipschitz continuous.

3) The effectiveness of this TSM (terminal sliding mode) based approach and the quasi-fixed-time convergence for different initial states are verified through both simulations and experiments.

The rest of this article is organized as follows. Problem formulation and some preliminaries are first introduced in Section II. The adaptive quasi-fixed-time integral terminal sliding mode control is investigated in Section III. Next, the proposed method is validated through both simulation and experiment in Section IV before the conclusion in Section V.

II. PROBLEM FORMULATION AND PRELIMINARIES

Consider an invertible nonlinear single input single output (SISO) system (see Chapter 4 in [18]) in the form of a chain of n-th order integrators:

$$
\begin{aligned}
\dot{x}_{i-1}(t) &= x_i(t), \ i = 2, \cdots, n \\
\dot{x}_n(t) &= \alpha(x) + \beta(x)u(t) + \varrho(x,t) \\
&= \alpha_0(x) + \beta_0(x)u + \underbrace{\tilde{\alpha}(x) + \tilde{\beta}(x)u + \varrho(x,t)}_{d(x,t)}
\end{aligned}
\tag{1}
$$

where the state $x(t) \in \mathbb{R}^n$, $u \in \mathbb{R}$ is the control input, $\alpha, \beta \in \mathbb{R}$ ($\beta \neq 0$) are the actual nonlinear models while α_0, β_0 ($\beta_0 \neq 0$) are the nominal ones; the residual term $\tilde{\alpha} = \alpha - \alpha_0$, etc., the lumped perturbation $d(x,t) \in \mathbb{R}$ is induced by model uncertainties $\tilde{\alpha}(x) + \tilde{\beta}(x)u$ and exogenous disturbances $\varrho(x,t)$.

In many literatures such as [2], [17], model uncertainties are not considered and an unreasonable constant bound of the lumped perturbation, even the bound on its derivative is directly given. However, one cannot estimate the actual bound of $d(x,t)$ in (1) before designing the controller $u(t)$. One of this brief's motivations is to eliminate the requirements on the prior knowledge of $d(x,t)$. The following assumption is made, as the designed controller $u(t)$ is generally based on the state feedback.

Assumption 1: The state $x(t)$ is fully measurable, $d(x,t)$ in (1) is continuously differentiable and bounded by

$$
|d(x,t)| \leq \bar{d}_0 + \bar{d}_1 \|x(t)\|^{m_1}
\tag{2}
$$

where $\bar{d}_0, \bar{d}_1$ are unknown bounded positive constants and $m_1 \in \mathbb{R}^+$ reflects the type of perturbation, e.g., $m_1 = 1$ for viscous friction in motor speed control [19] and $m_1 = 2$ for aerodynamic drags. If one has no prior knowledge of m_1, the default value $m_1 = 1$ is also acceptable.

Lemma 1: (see [16]) Given a system $\dot{x}(t) = f(x(t))$, if there exists a function $V(x) : \mathbb{R}^n \to \mathbb{R}^+ \cup \{0\}$ such that (I) $V(x) = 0 \Leftrightarrow x = 0$; (II) $\dot{V}(x) \leq -aV^{\rho_1}(x) - bV^{\rho_2}(x) + \delta$ for some $a, b > 0$ and $\rho_1 > 1$, $0 < \rho_2 < 1$, then for $\delta \in (0, \infty)$, state $x(t)$ is practically fixed-time stable with time $T \leq \frac{1}{a(\rho_1 - 1)} + \frac{1}{b(1 - \rho_2)}$, π is a scalar satisfying $0 < \pi < 1$.

$$
\lim_{t \to T} V(x) \leq \min \left\{ a^{-\frac{1}{\rho_1}} \left(\frac{\delta}{1 - \pi} \right)^{\frac{1}{\rho_1}}, b^{-\frac{1}{\rho_2}} \left(\frac{\delta}{1 - \pi} \right)^{\frac{1}{\rho_2}} \right\}
$$

Notations: For $x, \mu \in \mathbb{R}$, denote $\lceil x \rfloor^\mu = |x|^\mu \operatorname{sgn}(x)$ from now on for brevity, where $\operatorname{sgn}(x)$ is a signum function.

A saturation function is defined as below:

$$
\operatorname{sat}(x, \varphi) = x/\varphi, |x| \leq \varphi; \ \operatorname{sat}(x, \varphi) = \operatorname{sgn}(x), |x| > \varphi
\tag{3}
$$

III. ADAPTIVE QUASI-FIXED-TIME INTEGRAL TERMINAL SLIDING MODE CONTROL

To accomplish a quasi-fixed-time convergence of the dynamics in (1), the integral sliding manifold is designed as:

$$
s(t) = x_n + \int_{t_0}^t \sum_{i=1}^n k_i (\lceil x_i(\tau) \rfloor^{\mu_i} + \lceil x_i(\tau) \rfloor^{\nu_i}) d\tau
\tag{4}
$$

where k_i ($i = 1, \cdots, n$) makes the polynomial function of ψ ($\psi \in \mathbb{R}$), $\psi^n + k_n \psi^{n-1} + \cdots + k_2 \psi + k_1$ Hurwitz. Besides, μ_i (see [15]) can be chosen as follow:

$$
\mu_{i-1} = \frac{\mu_i \mu_{i+1}}{2\mu_{i+1} - \mu_i}, \ i = 2, \ldots, n, \ \forall n \geq 2
\tag{5}
$$

where $\mu_{n+1} = 1$, $\mu_n = \mu$, $0 < \mu_i < 1$ for $i = 1, \ldots, n$ and $\nu_i > 1$ is selected analogously (also can be found in [17]).

Before the introduction to *Theorem* 1, the following adaptive laws for the variable control gain $\hat{\eta}$ are defined in advance.

$$
\hat{\eta}(s(t)) = \begin{cases} \hat{\eta}_\alpha + \eta_1 |s|^{2\rho_1 - 1} + \eta_2 |s|^{2\rho_2 - 1}, & |s| > \bar{\varrho}_0 \\ \hat{\eta}_\beta, & |s| \leq \bar{\varrho}_0 \end{cases}
\tag{6}
$$

$$
\hat{\eta}_\alpha(s(t)) = \hat{d}_0(t) + \hat{d}_1(t) \|x(t)\|^{m_1}
\tag{7}
$$

$$
\dot{\hat{d}}_0(t) = \frac{1}{\theta_0} |s(t)| - \epsilon_0 \hat{d}_0(t)
\tag{8}
$$

$$
\dot{\hat{d}}_1(t) = \frac{1}{\theta_1} |s(t)| \|x(t)\|^{m_1} - \epsilon_0 \hat{d}_1(t)
\tag{9}
$$

$$
\hat{\eta}_\beta(s(t)) = \frac{(1 + \bar{\varrho}_0)\hat{\eta}_\alpha^\star + \eta_0}{\bar{\varrho}_0} \frac{|s(t)|}{|s(t)| + 1}
\tag{10}
$$

where $\hat{d}_0(t), \hat{d}_1(t) \in \mathbb{R}^+$ are the estimated gains w.r.t. the perturbation bound in (2), $\theta_0, \theta_1, \epsilon_0 \in \mathbb{R}^+$ are the design parameters and $\bar{\varrho}_0 \in \mathbb{R}^+$ is a small constant defined later in (18). In (6), design parameters $1 < \rho_1 < \infty, 1/2 < \rho_2 < 1, \eta_1, \eta_2 \in \mathbb{R}^+$ and in (10) $\eta_0 \in \mathbb{R}^+$ is a design parameter. Denote t_f^- as the time instant just before t_f, where $s(t_f) \leq \bar{\varrho}_0$ and $s(t_f^-) > \bar{\varrho}_0$, then $\hat{\eta}_\alpha^\star = \hat{\eta}_\alpha(s(t_f^-))$ is defined in (10).

Remark 1: In some literature like [20], $\hat{\eta}_\beta(s(t))$ is defined as a barrier function in the form as $\hat{\eta}_\beta(s(t)) = \frac{|s(t)|}{\bar{\varrho}_0 - |s(t)|}$ to generate a sufficient large gain when $s(t)$ approaches to $|s| = \bar{\varrho}_0$ from $s = 0$. Hence, this barrier function obviously leads to infinity ($|s| = \bar{\varrho}_0$) and high-frequency switch gains (see (6)), especially under measurement noises. In general, control signals are typically given to actuators rather than the plant in practical systems, and the actuators often possess limited bandwidth and cannot respond to high-frequency commands with large amplitudes. Hence, the conventional barrier function's high-frequency and large amplitude control gain can lead to a significant chattering phenomenon (see [21]). Therefore, a new nonsingular adaptive layer function is defined in (10) utilizing the continuously updated gain $\hat{\eta}_\alpha^\star$, which can adapt to the unknown varying perturbations and is chattering free. Intuitive results can be found in Section IV.

Theorem 1: The state $x(t)$ of nonlinear system (1) will converge into a vicinity of equilibrium in quasi-fixed-time, if the sliding manifold $s(t)$ is selected as (4) and the Lipschitz continuous control u is designed as follows:

$$u = \beta_0^{-1}(x)(u_{eq} + u_{sw}) \tag{11}$$

$$u_{eq} = -\alpha_0(x) - \sum_{i=1}^{n} k_i \left(\text{sat}(x_i, \varphi_i)|x_i|^{\mu_i} + \lceil x_i \rceil^{\nu_i} \right) \tag{12}$$

$$\mathcal{T}\dot{u}_{sw} + u_{sw} = -\hat{\eta}(s)\,\text{sgn}(s) \tag{13}$$

where $\hat{\eta}(s(t))$ is updated by (6), function $\text{sat}(x, \varphi)$ is defined in (3), φ_i is the small customizable boundary layer, k_i and $\mu_i, \nu_i (i = 1, \ldots, n)$ are constants that defined in (4) and (5); $\mathcal{T}$ is a small low pass filter constant, $\bar{\varrho}_0$ is induced by the saturation function in (3,12) and is defined later in (18).

Proof: *Stage 1:* When $|s(t)| > \bar{\varrho}_0$, $\hat{\eta}(s) = \hat{\eta}_\alpha(s) + \eta_1|s|^{2\rho_1-1} + \eta_2|s|^{2\rho_2-1}$ (6), choose the Lyapunov function as

$$V = \frac{1}{2}(s^2 + \theta_0 \tilde{d}_0(t)^2 + \theta_1 \tilde{d}_1(t)^2) \tag{14}$$

where $\tilde{d}_i(t) = \bar{d}_i - \hat{d}_i(t)$ ($i = 0, 1, \bar{d}_i$ see (2)), and $\tilde{d}_i, \hat{d}_i$ are utilized to represent $\tilde{d}_i(t), \hat{d}_i(t)$ for simplicity. Utilizing (1),(4),(6) and (11), $\dot{V}(t)$ can be derived as

$$\dot{V} = s\left[\alpha_0(x(t)) + \beta_0(x(t))u(t) + d(x,t) \right] \tag{15}$$

$$+ s\sum_{i=1}^{n} k_i(\lceil x_i(t) \rceil^{\mu_i} + \lceil x_i(t) \rceil^{\nu_i}) - \theta_0 \tilde{d}_0 \dot{\hat{d}}_0 - \theta_1 \tilde{d}_1 \dot{\hat{d}}_1$$

$$= -s(\hat{d}_0 + \hat{d}_1\|x\|^{m_1})\,\text{sgn}(s) + s(d(x,t) + \varrho_0(t) + o(\mathcal{T})) \tag{16}$$

$$- s(\eta_1|s|^{2\rho_1-1} + \eta_2|s|^{2\rho_2-1})\,\text{sgn}(s)$$

$$- \left[\tilde{d}_0 + \tilde{d}_1\|x(t)\|^{m_1} \right]|s(t)| + \epsilon_0\theta_0\tilde{d}_0\hat{d}_0 + \epsilon_0\theta_1\tilde{d}_1\hat{d}_1$$

where $\varrho_0(t)$ is defined by (17) due to the input (12) in order to reduce the chattering phenomenon under state measurement noises, since the derivative of $|x_i|^{\mu_i}$ is singular at $x_i = 0$ when $0 < \mu_i < 1$. Besides, $o(\mathcal{T})$ is induced by the low pass filter input in (13) and can be bounded by some constants (see [12]) since $\mathcal{T}$ is usually small. It will be proved later that these two treatments won't sacrifice the system robustness and at the same time, guarantee u in (11) is Lipschitz continuous.

$$\varrho_0(t) = \sum_{i=1}^{n} k_i \left(\text{sgn}(x_i) - \text{sat}(x_i, \varphi_i) \right)|x_i|^{\mu_i} \tag{17}$$

$$\bar{\varrho}_0 = \sup_{\bigcap |x_i| < \varphi_i} |\varrho_0(t)| \tag{18}$$

Since φ_i in (3) is small layer width, $\varrho_0(t), o(\mathcal{T})$ are both small, combine $\varrho_0(t) + o(\mathcal{T})$ (see 16) into the unknown term $\bar{d}_0$ of $|d(x,t)|$ (see (2)), and utilize (2,16) to obtain

$$\dot{V} \leq -(\eta_1|s|^{2\rho_1-1} + \eta_2|s|^{2\rho_2-1})|s(t)| \tag{19}$$

$$- (\hat{d}_0 + \hat{d}_1\|x(t)\|^{m_1})|s(t)| + (\bar{d}_0 + \bar{d}_1\|x(t)\|^{m_1})|s(t)|$$

$$- \left[\tilde{d}_0 + \tilde{d}_1\|x(t)\|^{m_1} \right]|s(t)| + \epsilon_0\theta_0\tilde{d}_0\hat{d}_0 + \epsilon_0\theta_1\tilde{d}_1\hat{d}_1$$

$$= -\eta_1 2^{\rho_1} \times (\frac{1}{2}s^2)^{\rho_1} - \eta_2 2^{\rho_2} \times (\frac{1}{2}s^2)^{\rho_2}$$

$$+ \epsilon_0\theta_0\tilde{d}_0(\bar{d}_0 - \tilde{d}_0) + \epsilon_0\theta_1\tilde{d}_1(\bar{d}_1 - \tilde{d}_1)$$

$$\leq -\eta_1 2^{\rho_1} \times (\frac{1}{2}s^2)^{\rho_1} - \eta_2 2^{\rho_2} \times (\frac{1}{2}s^2)^{\rho_2} \tag{20}$$

$$+ \frac{\epsilon_0\theta_0}{2}(\bar{d}_0^2 - \tilde{d}_0^2) + \frac{\epsilon_0\theta_1}{2}(\bar{d}_1^2 - \tilde{d}_1^2) \tag{21}$$

where the Young's inequality has been used in (21). Next some auxiliary terms are introduced into inequalities (20-21) and

$\eta_i^\circ = \eta_i 2^{\rho_i}$, $\eta_i' = \min\{\eta_i^\circ, 1\}$ $(i = 1, 2)$ are defined to obtain

$$\dot{V} \leq -\eta_1' \times \left[(\frac{1}{2}s^2)^{\rho_1} + (\frac{1}{2}\theta_0\tilde{d}_0^2)^{\rho_1} + (\frac{1}{2}\theta_1\tilde{d}_1^2)^{\rho_1} \right] \tag{22}$$

$$- \eta_2' \times \left[(\frac{1}{2}s^2)^{\rho_2} + (\frac{1}{2}\theta_0\tilde{d}_0^2)^{\rho_2} + (\frac{1}{2}\theta_1\tilde{d}_1^2)^{\rho_2} \right]$$

$$+ \frac{\epsilon_0\theta_0}{2}(\bar{d}_0^2 - \tilde{d}_0^2) + \frac{\epsilon_0\theta_1}{2}(\bar{d}_1^2 - \tilde{d}_1^2) + \eta_1^\circ(\frac{\theta_0}{2}\tilde{d}_0^2)^{\rho_1}$$

$$+ \eta_1^\circ(\frac{\theta_1}{2}\tilde{d}_1^2)^{\rho_1} + \eta_2^\circ(\frac{\theta_0}{2}\tilde{d}_0^2)^{\rho_2} + \eta_2^\circ(\frac{\theta_1}{2}\tilde{d}_1^2)^{\rho_2}$$

Next, since $\theta_i > 0$ in (8,9) and $1 < \rho_1, 1/2 < \rho_2 < 1$ defined under (10), using the fact that $\bar{d}_i^2 \geq \tilde{d}_i^2$, it can be obtained

$$\epsilon_0\frac{\theta_i}{2}\bar{d}_i^2 + \eta_2^\circ(\frac{\theta_i}{2}\tilde{d}_i^2)^{\rho_2} + \eta_1^\circ(\frac{\theta_i}{2}\tilde{d}_i^2)^{\rho_1} - \epsilon_0\frac{\theta_i}{2}\tilde{d}_i^2 \tag{23}$$

$$\leq \max \left\{ \begin{array}{ll} (\epsilon_0 + \eta_1^\circ)(\frac{\theta_i}{2}\bar{d}_i^2) + \eta_2^\circ(\frac{\theta_i}{2}\bar{d}_i^2)^{\rho_2}, & \frac{\theta_i}{2}\tilde{d}_i^2 < 1 \\ (\epsilon_0 + \eta_2^\circ)(\frac{\theta_i}{2}\bar{d}_i^2) + \eta_1^\circ(\frac{\theta_i}{2}\bar{d}_i^2)^{\rho_1}, & \frac{\theta_i}{2}\tilde{d}_i^2 \geq 1 \end{array} \right\} \triangleq \delta_i$$

Next, with Lemma 3 in [22], inequality in (23) and $\dot{V}$ in (22)

$$\dot{V} \leq -\eta_1' \times 3^{1-\rho_1}V^{\rho_1} - \eta_2' \times V^{\rho_2} + \delta_0 + \delta_1 \tag{24}$$

According to (14), $s(t)^2 \leq 2V$, $\theta_i\tilde{d}_i(t)^2 \leq 2V$ for $i = 0, 1$ are both satisfied. Then since V is bounded using *Lemma 1*, $|s(t)|, \sqrt{\theta_i}\tilde{d}_i(t)$ will converge in fixed-time as follow

$$\left\{ \sqrt{\theta_i}\tilde{d}_i(t), |s(t)| \right\} \leq 2^{\frac{1}{2}} \min \left\{ \left(\frac{\delta_0 + \delta_1}{\eta_1' 3^{1-\rho_1}} \right)^{\frac{1}{2\rho_1}}, \left(\frac{\delta_0 + \delta_1}{\eta_2'} \right)^{\frac{1}{2\rho_2}} \right\}$$

$$= 2^{\frac{1}{2}} \min \{ \delta_1', \delta_2' \} \tag{25}$$

Remark 2: According to (25), $s(t)$ could only converge into a vicinity of $s = 0$, which pays the price for the fixed-time perturbation estimation. Moreover, notice that $\bar{d}_1$ in (2, 23) is supposed to be small when the initial value $\|x(t_0)\|^{m_1}$ is very large. Otherwise, η_α, u, u_{sw} in (7,11,13) would exceed the control bound for real systems and the disturbance compensation becomes meaningless. The bounded input control problem is out of scope here and will be introduced in the future. Hence, there always exists proper small θ_0 in (23) such that $2^{\frac{1}{2}} \max \{ \delta_1', \delta_2' \} \leq \bar{\varrho}_0$ (see (18, 25)).

Stage 2: When $|s(t)| \leq \bar{\varrho}_0$, choose the Lyapunov candidate

$$V = \frac{1}{2}s^2 + \frac{1}{2}\hat{\eta}_\beta(s)^2 \tag{26}$$

utilizing (10) and the same treatment of $\varrho_0(t) + o(\mathcal{T})$ under (18), denote $\bar{d}(t) = \bar{d}_0 + \bar{d}_1\|x(t)\|^{m_1}$, it can be obtained that

$$\dot{\hat{\eta}}_\beta(s) = \frac{(1 + \bar{\varrho}_0)\hat{\eta}_\alpha^\star + \eta_0}{\bar{\varrho}_0} \frac{\text{sgn}(s)\dot{s}}{(|s| + 1)^2} = \frac{(1 + \bar{\varrho}_0)\hat{\eta}_\alpha^\star + \eta_0}{\bar{\varrho}_0(|s| + 1)^2}$$

$$\times \text{sgn}(s)\left[-\hat{\eta}_\beta(s)\,\text{sgn}(s) + d(x,t) + \varrho_0(t) + o(\mathcal{T}) \right]$$

$$\leq \frac{(1 + \bar{\varrho}_0)\hat{\eta}_\alpha^\star + \eta_0}{\bar{\varrho}_0(|s| + 1)^2} \left[-\hat{\eta}_\beta(s) + \bar{d}(t) \right] \tag{27}$$

then utilizing (1,4,11), the derivative of V in (26) w.r.t. time t can be derived as below:

$$\dot{V} = s\dot{s} + \hat{\eta}_\beta(s)\dot{\hat{\eta}}_\beta(s) \tag{28}$$

$$\leq s \left[-\hat{\eta}_\beta(s)\,\text{sgn}(s) + \bar{d}(t) \right]$$

$$+ \hat{\eta}_\beta(s) \times \frac{(1 + \bar{\varrho}_0)\hat{\eta}_\alpha^\star + \eta_0}{\bar{\varrho}_0(|s| + 1)^2} \left[-\hat{\eta}_\beta(s) + \bar{d}(t) \right]$$

$$\dot{V} \leq -\underbrace{\left[\, \hat{\eta}_\beta(s) - \bar{d}(t)\, \right]}_{\nu_1} |s| \tag{29}$$
$$-\hat{\eta}_\beta(s) \times \underbrace{\frac{(1+\bar{\varrho}_0)\hat{\eta}_\alpha^\star + \eta_0}{\bar{\varrho}_0(|s|+1)^2}}_{\nu_2} \left[\, \hat{\eta}_\beta(s) - \bar{d}(t)\, \right]$$

Define an intermediate term s_0 as (30), where $\eta_0 > 0$ is defined in (10). Notice the definition of $\hat{\eta}_\alpha^\star = \hat{\eta}_\alpha(s(t_f^-))$ under (10) and it has been proved in *stage 1* (see (7,25)) that the gain $\hat{\eta}_\alpha(s(t_f^-))$ will converge into a vicinity of $\bar{d}(t)$ in fixed-time. Hence, the inequality in (31) is valid with a proper η_0, and the monotonicity of the function $|s(t)|/|s(t)| + 1$ is utilized.

$$s_0 = \bar{\varrho}_0 \frac{\bar{d}(t)}{\bar{d}(t) + \eta_0/2} < \bar{\varrho}_0, \quad \bar{d}(t) > 0 \tag{30}$$

$$\hat{\eta}_\beta(s(t)) \geq \hat{\eta}_\beta(s_0) = \frac{(1+\bar{\varrho}_0)\hat{\eta}_\alpha^\star + \eta_0}{\bar{\varrho}_0(|s_0|+1)}|s_0|$$
$$= \left[(1+\bar{\varrho}_0)\hat{\eta}_\alpha^\star + \eta_0\right] \frac{\bar{d}(t)}{(1+\bar{\varrho}_0)\bar{d}(t) + \eta_0/2}$$
$$\geq \bar{d}(t), \quad s_0 \leq |s(t)| \leq \bar{\varrho}_0 \tag{31}$$

Hence, $\dot{V}$ in (29) can be scaled by $(\nu_1, \nu_2 > 0)$

$$\dot{V} \leq -\sqrt{2}\left\{\frac{\nu_1 |s|}{\sqrt{2}} + \frac{\nu_1 \nu_2 \hat{\eta}_\beta(s)}{\sqrt{2}}\right\} \leq -\sqrt{2}\min\{\nu_1, \nu_1\nu_2\}V^{\frac{1}{2}}$$

Hence, the sliding manifold finally converges into the small layer $|s(t)| \leq s_0$ within finite time (see [15]), combine (10) with (30), a larger η_0 ensures a smaller vicinity of $s(t) = 0$, but with the effort of a larger gain and vice-versa.

Stage 3: It has been proved in (31) that $|s(t)| \leq \bar{\varrho}_0$, for the small sampling time τ_s, it's known that $|\frac{s(t)-s(t-\tau_s)}{\tau_s}| \cong |\dot{s}(t)| \leq \bar{\varrho}_0/\tau_s$. Besides, $\dot{s}(t)$ in (4) has the same structure as in [17] and state x will converge into a small vicinity of zero in fixed-time, since $\bar{\varrho}_0/\tau_s$ can be regarded as a small inhomogeneous term of $\sum_{i=1}^n k_i(\lceil x_i(t) \rfloor^{\mu_i} + \lceil x_i(t) \rfloor^{\nu_i}) = 0$. Noticed that among these 3 stages, only in *stage 2*, $s(t)$ is finite-time stable. Hence, *Theorem 1* is completely proved.

IV. SIMULATION AND EXPERIMENT

Simulation 1. Consider a second-order nonlinear system as

$$\dot{x}_1 = x_2 \tag{32}$$
$$\dot{x}_2 = \cos(x_2) + (\,2 + \sin(x_2)\,)u(t) + \varrho(t)$$

where $\varrho(t) = \sin(5t) + \cos(4t)$ represents the unknown exogenous disturbance, $\alpha_0(x) = \cos(x_2)$ and $\beta_0(x) = 2 + \sin(x_2)$ are the nominal models in (1). The unknown actual model is set as $\alpha(x) = \cos(1.5x_2) + 0.5|x_2|^{0.25}$, $\beta(x) = 2.5 + \sin(x_2)$. The goal is to stabilize the system under the lumped perturbation and different initial states $x(t_0)$ in fixed time. The white noise with power $1e-8$ is added on $x(t)$ in (32).

Take an example, if the convergence time $T \leq 1.1s$ for $s(t)$ is set here, then $\rho_1 = 2, \rho_2 = 0.5, \eta_1 = 2, \eta_2 = 2$ in (6) can be designed accordingly using *Theorem* 1 and *Lemma* 1 (one can also refer to [4]), which leads to $T \leq 1.082s$. And control parameters $k_1 = 4, k_2 = 3, \mu_1 = \frac{9}{23}, \mu_2 = \frac{9}{16}, \nu_1 = \frac{21}{19}, \nu_2 = \frac{21}{20}$ in (4,5) can be designed similar to the procedure in Section II of [17]. Other parameters are selected as: $m_1 = 0.25$ in (7), $\theta_0 = 0.5, \theta_1 = 10, \epsilon_0 = 0.1$ in (8,9), $\eta_0 = 0.5$ in (10); and
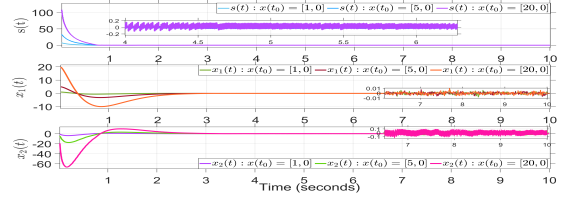

Fig. 1: Sliding manifold $s(t)$, state $x_1(t)$ and $x_2(t)$ with different initial states under the proposed nonsingular function $\hat{\eta}_\beta(s(t))$ in (10).
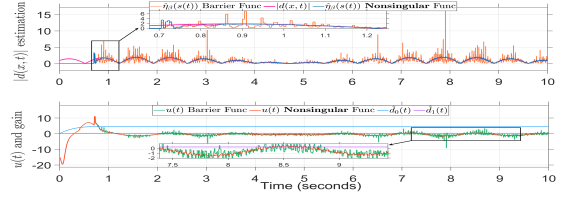

Fig. 2: Estimated gain $\hat{d}_0(t)$, $\hat{d}_1(t)$ and $u(t)$, $\hat{\eta}_\beta(t)$ under $x(t_0) = [1,0]$.

$\mathcal{T} = 0.02$ in (13); $\varphi_1 = 0.01, \varphi_2 = 0.02$ in (3). Three different initial states are given by $x(t_0) = [1,0], [5,0], [20,0]$.

Remark 3: As illustrated in Fig. 1, all the sliding manifolds $s(t)$ are driven into desired small vicinities of zero under the AFITSM in $T = 0.81s \leq 1.1s$ as analyzed above, despite the co-existence of model uncertainty and exogenous disturbance. Besides, all the states $x(t)$ converge into small vicinities of $x = (0,0)$ at $t = 3.1s$ simultaneously. These convergences are accomplished in quasi-fixed-time that is independent of the initial states. Meanwhile, in Fig. 2, under the proposed $\hat{\eta}_\beta(s)$ in (10), $\hat{d}_0, \hat{d}_1$ converge to the actual bound $\bar{d}_0, \bar{d}_1$ (see (2)) simultaneously from zero. Besides, when $s(t)$ converges into $\bar{\varrho}_0$ (see (31)), gain $\hat{\eta}_\beta$ dominates the controller (see (6)) and a non-switching $u(t)$ is generated due to the monotonicity of $\hat{\eta}_\beta$ w.r.t. $|s(t)|$ (see (10)), when $s(t)$ deviates from $s = 0$, $\hat{\eta}_\beta$ will increase monotonically and vice versa. System robustness isn't sacrificed since $\hat{\eta}_\beta(s) \geq \bar{d}(t)$ (see (31)), and this proof can be intuitively depicted in Fig.2, $\hat{\eta}_\beta(s)$ precisely estimates the lumped perturbation $|d(x,t)|$ while still insensitive to the measurement noises compared with the barrier function. The control signal generated by the barrier function is typically not feasible for real systems as analyzed in *Remark 1*.

Experiment 2. Consider the dynamics of a permanent magnet synchronous motor (PMSM) in [19].

$$\frac{d\omega}{dt} = \frac{3n_p\psi_{f0}}{2J_0}i_q - \frac{F_0}{J_0}\omega + d \tag{33}$$

where ω is the angular velocity, i_q is the q-axis stator current serves as the control input, n_p is the number of pole pairs, ψ_f is the flux linkage, J is the moment of inertia, F is the viscous friction coefficient, and their nominal values are: $n_p = 21, \psi_{f0} = 9.114e-3Wb, J_0 = 2.6e-4kg \cdot m^2, F_0 = 8e^{-6}(Nm \cdot s/rad)$. $s(t)$ is defined as (4) with $n = 1$ and $q_0 = 3n_p\psi_{f0}/2J_0$ is denoted. The lumped perturbation equals: ($\Delta J = J - J_0$, etc.)

$$d = \frac{3n_p(\Delta\psi_f J_0 - \Delta J\psi_{f0})}{2JJ_0}i_q - \frac{\Delta F J_0 - \Delta J F_0}{JJ_0}\omega - \frac{T_L}{J} \tag{34}$$

where T_L is the unknown time-varying load torque generated by the magnetic powder brake (see Fig. 4), and this load torque is proportional to the adjustable DC-voltage (see Fig.
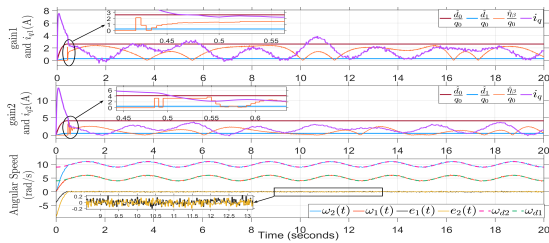
Fig. 3: top-middle: Gain estimation $\hat{d}_0, \hat{d}_1$ (q_0 is defined upon (34)), the current i_q. bottom: Tracking trajectory of the angular velocity ω and the tracking errors.
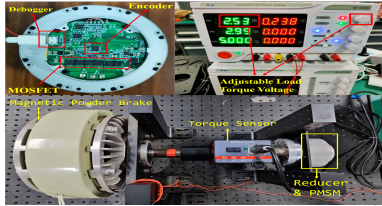

Fig. 4: Experiment platform and load torque generator.

4). Moreover, the tested PMSM is equipped with a reducer whose reduction gear ratio r_0 equals 10, and a low-cost chip AS5047 is selected to serve as the magnetic encoder (see Fig. 4). Besides, this PMSM is composed of 6 power MOSFETs (KNY3406C) and a motor drive DRV8301DCAR, the MCU is STM32F405VG and the sampling time is $\tau_s = 2$ms. Two desired angular velocities of the reducer shaft are set with $\omega_{d1} = 5$ - $\cos(\frac{4\pi}{5}t)$ rad/s and $\omega_{d2} = 10$ - $\cos(\frac{4\pi}{5}t)$ rad/s, the latter approaches the maximum speed of this PMSM, i.e., $11 \times r_0 \times 9.55 \approx 1100$ rpm. Due to the measurement noises of the encoder, the layer in (3) is expanded as $\varphi_1 = 0.2$ and $\theta_1 = 2$, $m_1 = 1$ due to the friction torque is proportional to ω (see (2,33)), other control parameters are not changed.

Remark 4: The converge time of the sliding manifold $s(t)$ and the gain estimation should be $T \leq 1.1$s as simulated above. In Fig. 3, although the initial tracking errors and the imposed unknown load torques (adjusted by the DC-Voltage) are quite different in the two tests, the angular velocity $\omega(t)$ and the gain estimation $\hat{d}_0, \hat{d}_1$ still converge simultaneously in quasi-fixed-time, about $T = 0.45$s ≤ 1.1s which verifies the correctness of the theorem. Besides, as depicted in Fig. 3, both two current signals i_q are smooth without chattering and singularities compared with the control signal under the barrier function in Fig. 2 and Fig. 15 in [20]. Finally, the root-mean-square tracking errors are 0.0712 for $\omega_1(t)$ and 0.0763 for $\omega_2(t)$, which reflects the perturbation estimation $\hat{\eta}_\beta(t)$ performs precisely. Otherwise, the errors $e_1(t), e_2(t)$ won't be that small without the perturbation compensation.

V. CONCLUSION

In this brief, a class of invertible nonlinear systems under the co-existence of model uncertainties and state-dependent disturbances is considered. An adaptive quasi-fixed-time integral terminal sliding mode control is developed to stabilize this system. The control input is chattering-free under the measurement noises and the prior information on the perturbation is not needed anymore. The adaptive fixed-time SMC problems under input saturation will be addressed in the future.

REFERENCES

[1] V. Utkin, "Variable structure systems with sliding modes," *IEEE Transactions on Automatic Control*, vol. 22, no. 2, pp. 212–222, Apr. 1977.

[2] Y. Feng, F. Han, and X. Yu, "Chattering free full-order sliding-mode control," *Automatica*, vol. 50, no. 4, pp. 1310–1314, Apr. 2014.

[3] N. Xavier and B. Bandyopadhyay, "Practical Sliding Mode Using State Depended Intermittent Control," *IEEE Transactions on Circuits and Systems II: Express Briefs*, vol. 68, no. 1, pp. 341–345, Jan. 2021.

[4] E. Moulay, V. Léchappé, E. Bernuau, and F. Plestan, "Robust Fixed-Time Stability: Application to Sliding-Mode Control," *IEEE Transactions on Automatic Control*, vol. 67, no. 2, pp. 1061–1066, Feb. 2022.

[5] A. Levant and B. Shustin, "Quasi-Continuous MIMO Sliding-Mode Control," *IEEE Transactions on Automatic Control*, vol. 63, no. 9, pp. 3068–3074, Sep. 2018.

[6] V. Utkin, "Discussion Aspects of High-Order Sliding Mode Control," *IEEE Transactions on Automatic Control*, vol. 61, no. 3, pp. 829–833, Mar. 2016.

[7] F. Plestan, Y. Shtessel, V. Brégeault, and A. Poznyak, "New methodologies for adaptive sliding mode control," *International Journal of Control*, vol. 83, no. 9, pp. 1907–1919, Sep. 2010.

[8] L. Liu, W. X. Zheng, and S. Ding, "An Adaptive SOSM Controller Design by Using a Sliding-Mode-Based Filter and its Application to Buck Converter," *IEEE Transactions on Circuits and Systems I: Regular Papers*, vol. 67, no. 7, pp. 2409–2418, Jul. 2020.

[9] H. Ma, Z. Xiong, Y. Li, and Z. Liu, "Sliding Mode Control for Uncertain Discrete-Time Systems Using an Adaptive Reaching Law," *IEEE Transactions on Circuits and Systems II: Express Briefs*, vol. 68, no. 2, pp. 722–726, Feb. 2021.

[10] Y. Chang, "Adaptive Sliding Mode Control of Multi-Input Nonlinear Systems With Perturbations to Achieve Asymptotical Stability," *IEEE Transactions on Automatic Control*, vol. 54, no. 12, pp. 2863–2869, Dec. 2009.

[11] Y. Yang, C. Hua, and J. Li, "A Novel Interaction Controller Design for Robotic Manipulators With Arbitrary Convergence Time," *IEEE Transactions on Circuits and Systems II: Express Briefs*, vol. 69, no. 4, pp. 2151–2155, Apr. 2022.

[12] C. Edwards and Y. B. Shtessel, "Adaptive continuous higher order sliding mode control," *Automatica*, vol. 65, pp. 183–190, Mar. 2016.

[13] S. Roy, S. Baldi, and L. M. Fridman, "On adaptive sliding mode control without a priori bounded uncertainty," *Automatica*, vol. 111, p. 108650, Jan. 2020.

[14] J. Ni, L. Liu, C. Liu, X. Hu, and S. Li, "Fast Fixed-Time Nonsingular Terminal Sliding Mode Control and Its Application to Chaos Suppression in Power System," *IEEE Transactions on Circuits and Systems II: Express Briefs*, vol. 64, no. 2, pp. 151–155, Feb. 2017.

[15] S. P. Bhat and D. S. Bernstein, "Geometric homogeneity with applications to finite-time stability," *Mathematics of Control, Signals, and Systems*, vol. 17, no. 2, pp. 101–127, Jun. 2005.

[16] A. Polyakov, "Nonlinear Feedback Design for Fixed-Time Stabilization of Linear Control Systems," *IEEE Transactions on Automatic Control*, vol. 57, no. 8, pp. 2106–2110, Aug. 2012.

[17] J. P. Mishra, X. Yu, and M. Jalili, "Arbitrary-Order Continuous Finite-Time Sliding Mode Controller for Fixed-Time Convergence," *IEEE Transactions on Circuits and Systems II: Express Briefs*, vol. 65, no. 12, pp. 1988–1992, Dec. 2018.

[18] A. Isidori, *Nonlinear Control Systems*, ser. Communications and Control Engineering, E. D. Sontag, M. Thoma, A. Isidori, and J. H. van Schuppen, Eds. London: Springer London, 1995.

[19] Y. A.-R. I. Mohamed, "Design and Implementation of a Robust Current-Control Scheme for a PMSM Vector Drive With a Simple Adaptive Disturbance Observer," *IEEE Transactions on Industrial Electronics*, vol. 54, no. 4, pp. 1981–1988, Aug. 2007.

[20] S. Mobayen, K. A. Alattas, and W. Assawinchaichote, "Adaptive Continuous Barrier Function Terminal Sliding Mode Control Technique for Disturbed Robotic Manipulator," *IEEE Transactions on Circuits and Systems I: Regular Papers*, vol. 68, no. 10, pp. 4403–4412, Oct. 2021.

[21] J. P. Mishra, X. Yu, and I. Boiko, "Frequency-Response of Non-Singular Terminal Sliding Mode Control With Actuators," *IEEE Transactions on Circuits and Systems II: Express Briefs*, vol. 69, no. 3, pp. 1392–1396, Mar. 2022.

[22] Q. Chen, S. Xie, and X. He, "Neural-Network-Based Adaptive Singularity-Free Fixed-Time Attitude Tracking Control for Spacecrafts," *IEEE Transactions on Cybernetics*, vol. 51, no. 10, pp. 5032–5045, Oct. 2021.